

## Decoupling of Structural and Electronic Phase Transitions in VO<sub>2</sub>

Zhensheng Tao, Tzong-Ru T. Han, Subhendra D. Mahanti, Phillip M. Duxbury, Fei Yuan, and Chong-Yu Ruan\*

*Physics and Astronomy Department, Michigan State University, East Lansing, Michigan 48824, USA*

Kevin Wang and Junqiao Wu

*Department of Materials Science and Engineering, University of California, Berkeley, California 94720, USA*

*and Division of Materials Sciences, Lawrence Berkeley National Laboratory, Berkeley, California 94720, USA*

(Received 11 June 2012; published 18 October 2012)

Using optical, TEM, and ultrafast electron diffraction experiments we find that single crystal VO<sub>2</sub> microbeams gently placed on insulating substrates or metal grids exhibit different behaviors, with structural and metal-insulator transitions occurring at the same temperature for insulating substrates, while for metal substrates a *new monoclinic metal phase* lies between the insulating monoclinic phase and the metallic rutile phase. The structural and electronic phase transitions in these experiments are strongly first order and we discuss their origins in the context of current understanding of multiorbital splitting, strong correlation effects, and structural distortions that act cooperatively in this system.

DOI: 10.1103/PhysRevLett.109.166406

PACS numbers: 71.30.+h, 61.50.Ks, 71.27.+a, 78.47.J-

The metal-insulator transition (MIT) is important in the general description of phase transitions in strongly correlated electron systems and in systems with various structural distortions [1]. Many transition metal oxides, including high-temperature superconductors and colossal magnetoresistive materials have broken orbital degeneracy that is tunable via structural symmetry, composition, and dimensionality, yielding numerous functional states that are close in free energy [2]. A prototypical system, vanadium dioxide (VO<sub>2</sub>) exhibits similar complexities as it transforms from a rutile (*R*) metal into a monoclinic (*M1*) insulator at a critical temperature near room temperature ( $T_c \approx 340$  K) as described in Fig. 1(a). The structural and MIT transitions in VO<sub>2</sub> are frequently observed to occur at the same temperature and have been extensively studied by x-ray [3–6], optical [7–10], THz [11,12], photoemission [13], and electron diffraction [14] techniques. However, several observations of distinct MIT and structural phase transitions (SPT) have been reported. These fascinating results are difficult to interpret as alternative mechanisms such as the coexistence of metal and insulating states, strain induced nanostructures, or filamentary current-induced MITs may be at play in these experiments. Here we show that the transition temperatures of the strongly first-order MIT and SPT in VO<sub>2</sub> microbeams may be separated by simply changing the substrate from insulator to metal. In our experiments single crystal VO<sub>2</sub> microbeams are gently placed on either insulating substrates or on metal TEM grids in order to minimize strain effects, nevertheless, on both gold and copper grids we find a strong splitting of the MIT and monoclinic to rutile phase transitions.

There has been extensive debate over the cause and effect relationship of the VO<sub>2</sub> MIT, involving Peierls [15], spin-Peierls [16], and Mott-Hubbard [17] scenarios. Density functional theory and single site dynamical mean field

theory (DFT + DMFT) calculations suggest a Mott-Hubbard MIT [18], while the recent cluster DMFT calculations find spin-singlet formation enhanced by strong Coulomb interactions [19]. Moreover, the most recent cluster DFT + DMFT calculations [20] indicate that the predominant *d* orbitals participating in a Peierl's dimerization along the *z* axis are the *xz* and *yz* orbitals instead of the *xy* orbitals as put forward by Goodenough [15] and elucidated

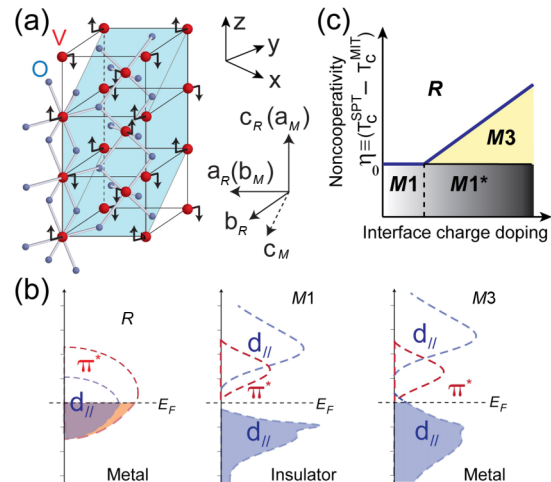


FIG. 1 (color online). (a) VO<sub>2</sub> rutile and monoclinic (*M1*) lattice structures. (b) Band structures of VO<sub>2</sub> in different phases. The left and middle panels are schematically drawn following Refs. [15,20]. The right panel describes proposed band structure for the monoclinic metal (*M3*). (c) VO<sub>2</sub> phase diagram as a function of temperature and interface charge doping. The vertical axis is the noncooperativity ( $\eta$ ), which measures the upshift of structural critical temperature ( $T_c^{\text{SPT}}$ ) from the electronic one ( $T_c^{\text{MIT}}$ ). The vertical dotted line indicates that the *M1\** regime may evolve smoothly from the *M1* phase as charge doping increases.

in many subsequent studies [21]. Occupancy of the Peierls bonding band in the insulating phase is then close to 2 instead of 1 as in a Goodenough-type analysis, reconciling the Peierls picture with recent x-ray absorption [4,13] and photoemission [13] studies identifying a large spectral weight transfer from  $\pi^*(d_{xy})$  into the valence  $d_{\parallel}(d_{xz,yz})$  orbitals following the pairing transition [Fig. 1(b)]. Meanwhile,  $\text{VO}_2$ 's remarkable electrical and optical switching properties (up to 2 orders of magnitude) [22] have inspired numerous applications including optoelectronics, data storage, bolometry, and smart windows [23], making understanding of the fundamental physics of the  $\text{VO}_2$  phase transitions a tremendously rewarding yet challenging task.

We define noncooperativity ( $\eta$ ) as the upshift of the critical temperature of the structural phase transition ( $T_c^{\text{SPT}}$ ) from that of the metal-insulator transition ( $T_c^{\text{MIT}}$ ) which is induced by metal interfaces, that we propose is due to charge transfer from the substrate into the  $\text{VO}_2$  itinerant orbitals thus affecting the critical condition for the Peierls transition. Surprisingly, the MIT remains nearly unaffected by this interface charge doping, as schematically illustrated in Fig. 1(c). To demonstrate splitting of the SPT from the MIT we use single-crystal  $\text{VO}_2$  microbeam samples with very few defects, grown using vapor transport deposition [24,25]. The importance of phase coexistence and nanoscale spatial growth of electronic inhomogeneities, found in multigrain thin films, is informative of the correlated nature of MIT [7], and similar competitive phase coexistence has been identified in single-crystal microbeams under strain [8,24,25], whereas without strain, sharp transitions were observed. Here, to minimize the strain effects, the microbeams ( $\approx 100$  to  $500$  nm laterally) are freely suspended on a Si window or on transmission electron microscope (TEM) grids of different metals. These sample geometries yield strongly first-order phase transitions as revealed by optical microscopy, where the color contrast tracks the optical reflectivity that varies drastically during the MIT [24–26]. Figure 2(b) shows that the first-order MIT at  $T_c^{\text{MIT}} = 339$  K leads to a sharp jump in the brightness as the sample is heated through the MIT. Observation of the diffraction pattern of the microbeam under TEM (JEOL 2200FS) as the sample is heated yields the results of Fig. 2(c), showing that the dimer reflections ( $S_1$ ), such as  $(1\ 0\ 1)$ ,  $(1\ 0\ 0)$ , and  $(1\ 0\ \bar{1})$ , disappear beyond  $T_c^{\text{SPT}}$  (344 K on a Ni TEM grid), when monoclinic  $\text{VO}_2$  turns into the more symmetric rutile structure through unpairing of V atoms along the  $c_R$  axis.

Measurements of MIT and SPT for several systems are reported in Fig. 2(d), showing that  $T_c^{\text{SPT}}$  upshifts from  $T_c^{\text{MIT}}$  by different amounts on different metallic grids, whereas on Si the SPT and MIT critical temperatures are approximately equal (339 K, see Supplemental Material [26] for details). While difficult to separate structurally, the different phases [ $M1^*$ ,  $M1$ , and  $M3$  as illustrated in Fig. 1(c)] are

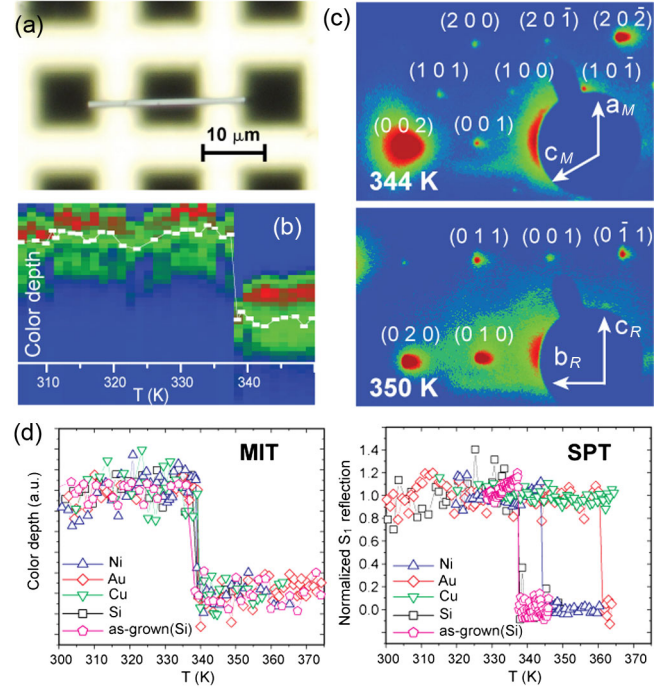


FIG. 2 (color online). (a) Optical image of a  $\text{VO}_2$  microbeam suspended on a TEM window. (b) Color depth change in the optical image of  $\text{VO}_2$  associated with a first-order insulator-to-metal transition at 339 K. (c) TEM diffraction patterns obtained from a  $\text{VO}_2$  microbeam suspended over a Ni TEM grid showing a monoclinic-to-rutile structural transition at 344 K. (d) Various metal-insulator transitions (MIT) and structural phase transitions (SPT) characterized over different metal TEM grids (Ni, Au, Cu), on a Si window, and in the as-grown condition where the microbeam is anchored on a Si substrate.

distinguishable by their optical properties, although the MIT between  $M1^*$  and  $M3$  has no discernable lattice symmetry change. The new monoclinic metal ( $M3$ ) phase, and the  $M1^*$  regime that evolves from the  $M1$  phase as interface-mediated charge doping enhances the Peierls coupling, emerge on a metal grid and are different from the strain [8,24] or chemical-doping stabilized  $M2$  [23] or triclinic ( $T$ ) phase, which has a larger unit cell and lies between  $M1$  and  $R$  phases [3,17].

We find that changing the substrate of the  $\text{VO}_2$  nano-beams impacts the critical condition for lattice dimerization significantly; however, it does little to influence the MIT. We attribute the upshift of  $T_c^{\text{SPT}}$  on metal substrates to a charge doping effect mediated by charge injection through the metal contact into  $\text{VO}_2$ . In a rigid band picture, initially these charges will go to the  $\pi^*$  band, making the interface metallic. To screen the injected charges a Debye sheath will be induced to prevent further charge injection, so the charge doping effect will be limited in the interface region ( $\approx 10$ – $100$  nm) [27]. However, we have observed a consistent upshift of  $T_c^{\text{SPT}}$  throughout the microbeam. In light of the current theoretical picture where both Mott and Peierls physics are involved [19,20], we suggest that the

injection of charge into the  $\pi^*$  band renormalizes the spectral functions [4,13] through local shifts in the Hartree energies ( $\approx 0.5$  eV) such that the  $d$  component of the spectral character of the upper valence band increases to accommodate these extra electrons, thereby preserving the gap and the insulating nature of the  $M1^*$  phase, and this emanates throughout the microbeam [26]. In this process the bonding  $d$  character is increased, leading to an enhancement of the bonding-antibonding Peierls gap, thus increasing the Peierls transition temperature (compared to the  $M1$  phase). The existence of the  $M3$  phase and the transition from  $M1^*$  to  $M3$  is primarily driven by Mott physics.

Further information concerning the underlying physics of the MIT and SPT in  $\text{VO}_2$  has been revealed by recent ultrafast pump-probe studies of  $\text{VO}_2$  films where an optically stimulated transient nonadiabatic insulator-metal transition within the monoclinic structure has been identified. The application of femtosecond (fs) laser pulses allows rapid excitation of electron-hole pairs from the insulating ground state, effectively driving a transition to the metallic state while the Peierls pairing is still intact. Even at fluences below what would be required to produce a high-symmetry structure, ultrafast reflectivity [9] and THz spectroscopy [11,12] measurements identified coherent phonon modulations near 6 THz in  $\text{VO}_2$  films, better associated with a transient metallic phase. Most of these studies also demonstrated a threshold behavior in the onset of sub-ps dynamics [11,12,14]. The existence of a critical threshold in the photoinduced structural phase transition [28] is considered to be the hallmark of a density-driven nonlinear conversion process that may involve strong electron-electron interactions. Meanwhile, the critical thresholds established in these film experiments (ranging from 4 to  $7 \text{ mJ cm}^{-2}$ ) are consistent with the free energy requirement for an  $M1$ - $R$  transition, suggesting that the critical threshold may be limited by a structural bottleneck [9].

We used ultrafast electron crystallography (UEC) experiments [29] to investigate optically driven dynamics of single-crystal  $\text{VO}_2$  microbeams in different fluence and temperature regimes. We started with studies of the undoped as-grown  $\text{VO}_2$  microbeams [Fig. 3(a)] where we applied a 50 fs near-infrared (800 nm) pulse to illuminate the full microbeam, followed by a sequence of probe electron pulses focused near the tip of the beam to track the lattice transformations that are expected to strongly couple to carrier excitations. As shown in Fig. 3(b), a full scale  $M1$ -to- $R$  transition can be stimulated by fs laser pulses. The SPT is tracked from the disappearance of dimer reflections ( $S_1$ ):  $(5\ 1\ \bar{2})$ ,  $(3\ 0\ \bar{1})$ ,  $(1\ \bar{1}\ 0)$ , which occurs when the applied fluence ( $F$ ) exceeds a critical value ( $F_c$ ). Figure 3(c) shows a laser induced first-order SPT occurring at  $F_c = 0.59 \text{ mJ cm}^{-2}$  with  $\text{VO}_2$  held at a base temperature ( $T_B$ ) of 325 K. To determine whether this threshold is density or

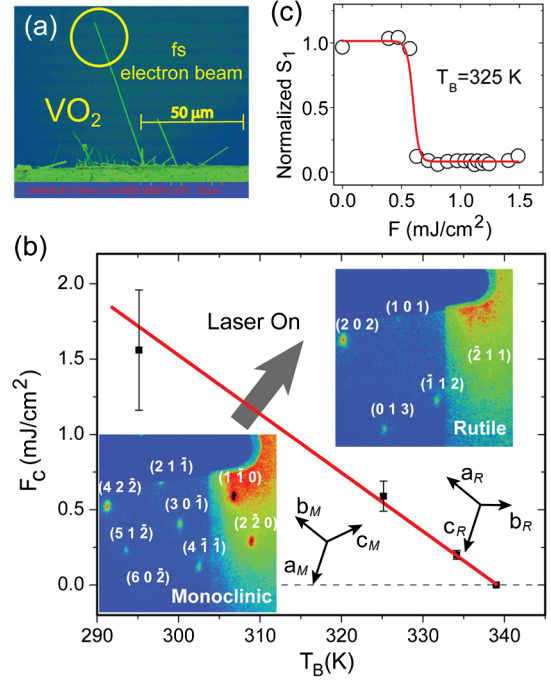


FIG. 3 (color online). (a) The SEM image of  $\text{VO}_2$  microbeams grown on a Si substrate. (b) The critical fluence ( $F_c$ ) for inducing the monoclinic-to-rutile transition as a function of base temperature  $T_B$ . The insets show the corresponding UEC patterns of the two phases. (c) The threshold behavior of the laser induced phase transition, as characterized by the disappearance of the dimer reflections ( $S_1$ ).

thermally driven, we examine  $F_c$  at different base temperatures, starting from around  $T_c \approx 339$  K where SPT occurs spontaneously. We observe a linear increase of  $F_c$  as  $T_B$  deviates from  $T_c$  as shown in Fig. 3(b), suggesting that laser-induced SPT can be described by crossing of the free energies from  $M1$  to  $R$ . To confirm this, we equate the absorbed optical energy  $E_{\text{ph}} = F_c/d$  ( $d$  is the optical penetration depth in  $\text{VO}_2$ ) to the thermodynamical energy:  $E_{\text{ph}} = -C_v(T_B - T_c) + H_L$ , where  $C_v$  and  $H_L$  are the specific and latent heats, respectively. From our fit, we find  $C_v = 3.2 \pm 0.2 \text{ J K}^{-1} \text{ cm}^{-3}$ , consistent with the previously established  $C_v = 3.1 \text{ J K}^{-1} \text{ cm}^{-3}$  [22] for  $M1$ - $\text{VO}_2$  (using  $d = 127$  nm for  $M1$  [5]), and  $H_L \approx 0$ . We find that below  $F_c$  the lattice fluctuations as characterized by the atomic displacement variance (see discussion below) are reversible, whereas above  $F_c$  the  $R$  state did not revert to  $M1$  within the pump-probe cycle of 1 ms. This intriguing result may be explained based on a Mott-driven, Peierls-limited structural phase transition consistent with recent near-infrared optical microscopy experiments, which indicate that the transition occurs via nucleation of the nanoscale correlated metallic puddles within the microcrystalline insulating  $\text{VO}_2$  host [7]. Observed here is a temporal hysteresis (supercooling) [26] known to associate with the rutile metallic phase that at  $F > F_c$  grows from nanoscale puddles

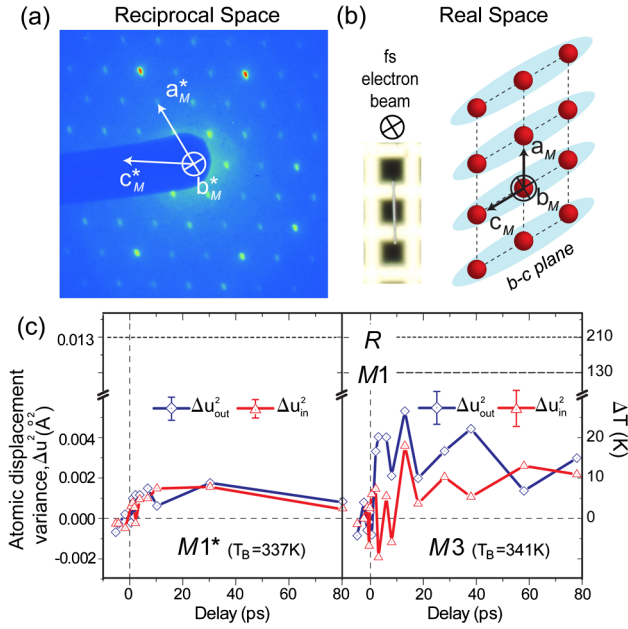


FIG. 4 (color online). (a) UEC pattern over suspended  $\text{VO}_2$  microbeam, showing reciprocal lattice of the  $ac$  plane of monoclinic structure. (b) The corresponding real space arrangement depicted with V sublattice. The fs electron beam is directed along  $b_M$ . (c) Lattice fluctuational dynamics in the  $M1^*$  and  $M3$  states are measured by the projected atomic displacement variance:  $\Delta u_{\text{out}}^2$  (along  $a_M^*$ , out-of- $bc$ -plane vibration), and  $\Delta u_{\text{in}}^2$  (in- $bc$ -plane vibration). The corresponding temperature increases expected from the  $M1$  and  $R$  phases are plotted for comparison.

to produce a SPT for the full microbeam over many cycles, removing  $H_L$  from the threshold requirement. We also conducted UEC on  $\text{VO}_2$  beams suspended over a Si TEM window and found similar critical fluences, albeit the suspended  $\text{VO}_2$  occasionally reorients itself after the SPT. Since enthalpy is dominated by the lattice component, these results support the hypothesis that the cooperative (SPT and MIT at the same temperature) phase transition has a strong Peierls character.

Now we use Au-supported microbeams and direct the fs electron beam along the monoclinic  $b$  axis [Figs. 4(a) and 4(b)] to study the optically stimulated responses from  $M1^*$ , concentrating on results found by setting  $T_B = 337$  K, which is just 2 K below  $T_c^{\text{MIT}}$ . In stark contrast to the undoped case, no SPT into  $R$  can be observed up to  $F = 7$   $\text{mJ cm}^{-2}$ , which has already exceeded the  $F_c \approx 3$   $\text{mJ cm}^{-2}$  for the  $M1$ -to- $R$  transition for the same  $T_B$  even considering  $H_L$  [5, 11]. This suppression is consistent with the upshift of the critical temperature of SPT. From time-dependent Debye-Waller (DW) analysis, we deduce the induced mean atomic displacement variance ( $\Delta u^2$ ) to be less than  $0.0015 \text{ \AA}^2$  at  $F = 7$   $\text{mJ cm}^{-2}$  as shown in Fig. 4(c). In comparison, our investigation of  $M3$ , conducted by setting  $T_B = 341$  K, shows a sizeable increase in the fluctuational response (also at  $F = 7$   $\text{mJ cm}^{-2}$ ). This

increase is reminiscent of the anomalously large DW factors identified in the metallic rutile phase in the earlier x-ray experiments, suggesting a lattice softening in the metallic state [3, 26]. Using the DW metric deduced from X-ray experiments the  $\Delta u^2$  increase at  $M3$  corresponds to a temperature rise ( $\Delta T$ ) of no more than 20 K [26], which is significantly less than the predictions for  $M1$  and  $R$  phases [see Fig. 4(c)]. The strong reduction in the absorbed energy can be understood based on an upshift in optical band gap, which, consistent with the increase of the Peierls transition temperature, leads to a strong reduction in optically accessible spectral weight compared to that in the cooperative  $M1$ - $R$  transition. The persistence of a large Peierls gap in  $M3$  is a clear evidence that the insulator-metal transition involves only a small portion of the spectral weight and the low energy spectra near FS [Fig. 1(c)]. We also establish that the spectral function adjustment associated with the MIT may be coupled to a soft phonon mode that favors the lattice distortion along  $a_M^*$ -shown by the suppression of  $\Delta u_{\text{in}}^2$  (in- $bc$ -plane vibration) relative to  $\Delta u_{\text{out}}^2$  (out-of- $bc$ -plane vibration) in Fig. 4(c).

In conclusion, we have shown the first clear evidence that the critical temperature associated with the Mott instability is lower than the structural phase transition temperature. We also observe a new monoclinic metallic phase ( $M3$ ), which we show may be stabilized by charge doping [6, 30]. Informed by our ultrafast single-beam measurements, the metal-insulator transition in the undoped case can be classified as Mott-driven, Peierls-limited, where the imposed cooperativity is mainly governed by the large spectral weight and the high energy scale inherent to the Peierls transition and that such stabilizing features are subjective to the strong Coulomb interaction predominant only in the insulating state without doping [20]. We also uncover the unique delocalized nature of the interface-mediated charge doping effect that can be rationalized with an active spectral weight transfer from the unfilled band to the Peierls band in the monoclinic structure, which enhances the Peierls interaction supported by its selective effect on the structure phase transition temperature. While the results presented here are very specific, they are generally compatible with the Peierls-Mott scenario proposed by most recent theories [19, 20], and amazingly reconcilable with an array of different experiments supportive of either Peierls or Mott scenarios. It would be extremely interesting for future orbital-selective experiments to address the electron correlations associated with  $M3$  in the near gap region. We expect the findings presented here will have important ramifications in bringing forth a unified understanding of the general MIT problems in strongly correlated materials.

Research at Michigan State University is supported by Department of Energy under Grant No. DE-FG02-06ER46309. J.W. acknowledges support from the National Science Foundation under Grant No. ECCS-1101779.

- \*Corresponding author.  
ruan@pa.msu.edu
- [1] M. Imada, A. Fujimori, and Y. Tokura, *Rev. Mod. Phys.* **70**, 1039 (1998).
- [2] E. Dagotto, *Science* **309**, 257 (2005).
- [3] D. B. McWhan, M. Marezio, J. P. Remeika, and P. D. Dernier, *Phys. Rev. B* **10**, 490 (1974).
- [4] M. W. Haverkort *et al.*, *Phys. Rev. Lett.* **95**, 196404 (2005).
- [5] A. Cavalleri, Cs. Tóth, C. Siders, J. Squier, F. Ráksi, P. Forget, and J. Kieffer, *Phys. Rev. Lett.* **87**, 237401 (2001).
- [6] B.-J. Kim, Y. W. Lee, S. Choi, J.-W. Lim, S. J. Yun, H.-T. Kim, T.-J. Shin, and H.-S. Yun, *Phys. Rev. B* **77**, 235401 (2008).
- [7] M. M. Qazilbash *et al.*, *Science* **318**, 1750 (2007).
- [8] A. C. Jones, S. Berweger, J. Wei, D. Cobden, and M. B. Raschke, *Nano Lett.* **10**, 1574 (2010).
- [9] A. Cavalleri, Th. Dekorsy, H. H. W. Chong, J. C. Kieffer, and R. W. Schoenlein, *Phys. Rev. B* **70**, 161102R (2004).
- [10] H.-T. Kim, Y. W. Lee, B.-J. Kim, B.-G. Chae, S. J. Yun, K.-Y. Kang, K.-J. Han, K.-J. Yee, and Y.-S. Lim, *Phys. Rev. Lett.* **97**, 266401 (2006).
- [11] C. Kübler, H. Ehrke, R. Huber, R. Lopez, A. Halabica, R. F. Haglund, and A. Leitenstorfer, *Phys. Rev. Lett.* **99**, 116401 (2007).
- [12] D. J. Hilton, R. P. Prasankumar, S. Fourmaux, A. Cavalleri, D. Brassard, M. A. El Khakani, J. C. Kieffer, A. J. Taylor, and R. D. Averitt, *Phys. Rev. Lett.* **99**, 226401 (2007).
- [13] T. C. Koethe *et al.*, *Phys. Rev. Lett.* **97**, 116402 (2006).
- [14] P. Baum, D.-S. Yang, and A. H. Zewail, *Science* **318**, 788 (2007).
- [15] J. B. Goodenough, *J. Solid State Chem.* **3**, 490 (1971).
- [16] D. Paquet and P. Leroux-Hugon, *Phys. Rev. B* **22**, 5284 (1980).
- [17] A. Zylbersztein and N. F. Mott, *Phys. Rev. B* **11**, 4383 (1975).
- [18] M. S. Laad, L. Craco, and E. Muller-Hartmann, *Phys. Rev. B* **73**, 195120 (2006).
- [19] S. Biermann, A. Poteryaev, A. I. Lichtenstein, and A. Georges, *Phys. Rev. Lett.* **94**, 026404 (2005).
- [20] C. Weber, D. D. O'Regan, N. D. M. Hine, M. C. Payne, G. Kotliar, and P. B. Littlewood, *Phys. Rev. Lett.* **108**, 256402 (2012).
- [21] V. Eyert, *Ann. Phys. (Leipzig)* **11**, 650 (2002).
- [22] C. N. Berglund and H. J. Guggenheim, *Phys. Rev.* **185**, 1022 (1969).
- [23] L. Whittaker, C. J. Patridge, and S. Banerjee, *J. Phys. Chem. Lett.* **2**, 745 (2011).
- [24] J. Cao *et al.*, *Nature Nanotech.* **4**, 732 (2009).
- [25] J. Wei, Z. Wang, W. Chen, and D. H. Cobden, *Nature Nanotech.* **4**, 420 (2009).
- [26] See Supplemental Material at <http://link.aps.org/supplemental/10.1103/PhysRevLett.109.166406> for extended results on the phase transitions, the temperature calibration, and further details on the analyses of the experimental results.
- [27] T. Mueller, F. Xia, M. Freitag, J. Tsang, and Ph. Avouris, *Phys. Rev. B* **79**, 245430 (2009).
- [28] K. Yonemitsu and K. Nasu, *Phys. Rep.* **465**, 1 (2008).
- [29] C.-Y. Ruan, Y. Murooka, R. K. Raman, R. A. Murdick, R. J. Worhatch, and A. Pell, *Microsc. Microanal.* **15**, 323 (2009).
- [30] S. Zhang, J. Y. Chou, and L. J. Lauhon, *Nano Lett.* **9**, 4527 (2009).